Dear Reviewer,

We appreciate your careful consideration of our manuscript. We have carefully responded to all of your **point-by-point** comments and issues and have revised the manuscript accordingly. These revisions are described in detail below.

Reviewer #2

This paper presents an analysis of measurements of gas-phase nitrous acid (HONO), and related air pollutants/atmospheric chemical species, performed in the boundary layer in Beijing prior to and during the Covid-19 lockdowns in early 2020. The variation in abundance of HONO, its precursors and related species are used to quantify different chemical source and sink terms for HONO, and from their diurnal variation and change across the start of lockdown, inferences drawn re their relative importance – in particular direct vehicle emission.

The abundance and sources of HONO are very much a current topic in urban atmospheric chemistry/air pollution, as besides being a pollutant in its own right HONO is usually the major precursor to (reservoir for) the key oxidant OH. Lockdown presents a unique near-step-change opportunity to explore these processes. This paper adds to the developing understanding of these sources, and in that respect is a valuable contribution to the literature.

The measurements appear to have been carefully performed and are clearly presented, and the analysis is interesting, with clear signal in the change in mean diurnal variations (which are used to develop qualitative arguments).

However, I have substantial reservations about several key assumptions/aspects of the quantitative analysis approach, which in my opinion do not allow the authors to draw the conclusions they reach. These are:

Response: Thanks for your positive comments and good suggestions. We will reply to your concerns point-by-point below.

Major comments

1. Meteorology. Obviously, weather changes affect pollutant advection, import,

dispersion, chemical processing, etc. The paper presents "before" vs "after" comparisons of concentrations either side of the start of lockdown, without consideration (beyond a basic vertical dispersion parameterization) of these effects. There is significant literature on the importance of correcting for meteorology–for example applying de-weathering approaches – several using the specific example of air pollutant abundance in Beijing across lockdown (e.g. Jiabo et al., 2021; Shi et al., 2021; Lv et al., 2022). How much of the observed change (or lack of change) in each species is due to changes in the weather between the two time periods P1 and P2? It would be interesting to repeat the analysis using deweathered concentrations.

Response: Thank you for your good comments and suggestions. We agree with you that meteorology is always one of the important factors affecting the concentration of air pollutants. As you suggested, we performed the de-weather analysis using a Random Forest model with a deweather module.

In lines 345-369 in the revised manuscript, we added a paragraph "It is worth noting that changes in atmospheric pollutant concentrations are affected by both emissions and meteorology. Especially, during the lockdown period, meteorological conditions in Beijing were not conducive to the dispersion of pollutants, thus the impact of meteorological conditions on the concentration of these pollutants needs to be assessed. We use the random forest algorithm of machine learning to remove the influence of meteorology from air quality time series data by a deweather method. The details are present in Text S1 in the SI. The model performs well in predicting the concentrations of pollutants compared to the observations in both the training and test datasets (Table S5). The concentrations and relative changes of each pollutant after deweather are recorded in Table S6. After deweather, the mean concentration of $PM_{2.5}$ increased significantly from 45.22±28.56 in P1 to 67.92±57.97 μg m^{-3} in P2 at a confidence level of 0.05, with an increase of 50.2%; The mean concentration of HONO was 0.89±0.37 ppb in P1, while it decreased to 0.51±0.25 ppb in P2, with a drop of 42.70%; The concentrations of NO and NO_2 significantly decreased from 15.44±18.40 and 23.28±7.28 ppb in P1 to 3.24±2.05 and 16.43±5.98 ppb in P2, respectively, which decreased by 79.02% and 29.42% respectively; SO_2 decreased from 2.27±0.69 in P1 to

1.48±1.18 ppb in P2, a decrease of approximately 34.8%; CO increased from 823.60±318.92 in P1 to 896±488.29 ppb in P2 (an increase of 8.79%) and O_3 increased from 16.98±5.62 to 22.60±4.10 ppb, an increase of about 33.1%, which was much lower than the change range of observed values (75.08%). As shown in Table S6, meteorological conditions have a significant impact on O_3 concentration. The impact was +39.64% and +6.15% in P1 and P2, respectively. The impact of deweather on NO in the two periods was -16.18% and +32.79%, respectively. It was -13.75% and -4.81%, respectively, for NO_2. However, the changes of other species in the two periods after deweather fluctuated between 2.3% and 7.8%. This implies that meteorological conditions have an important impact on the concentrations of NO and O_3, while meteorological factors have little impact on HONO, SO_2, CO and $PM_{2.5}$."

In lines 421-423 in the revised manuscript, we added the sentence "After deweather, the HONO concentration decreased significantly from 0.89±0.37 in P1 to 0.51±0.25 ppb in P2 at a confidence level of 0.05, with a decrease of 42.7%. This means that meteorology has little impact on HONO."

In the revised SI, we added the details about the random forest model to correct the influence of meteorology, including an introduction to the algorithm, a flow chart, and a model evaluation. The added content is as follows:

Text S1 De-weather model

Changes in atmospheric pollutant concentration are affected by emissions and meteorology. Machine learning models, including boosted regression trees and random forest (RF) algorithms, often exhibit higher predictive accuracy because of their advantages in modeling complex relationships between response variables and predictor variables (Zhan et al., 2018). By reducing the variance/bias and error of high-dimensional data sets, it has better performance compared to traditional statistical and air quality models. The algorithm resolves the relationship between air pollutant levels and their predictors, including meteorological parameters and time variables such as the day of the year (Julian Day), day of the week (Monday to Sunday), and hour of the day (0-23) (Grange et al., 2018). The input data set was randomly divided into a training data set for building the RF model (i.e., 70% of the input data set) and a testing data set

(30% of the input data set) for testing the performance of the RF model using unseen data sets. The RF model is an ensemble model composed of many individual decision tree models (Breiman, 2001).

In the RF model, the bagging algorithm is utilized, which involves randomly selecting samples from the training dataset, with replacement, along with their respective predictor features. Each decision tree is grown based on various decision rules that optimize the fitting between observed pollutant concentrations (response variable) and their predictor features. The selection of predictor features for each tree node is performed randomly to achieve the best possible split. The predicted pollutant concentrations are determined by aggregating the outcomes of all individual decision trees through a weighted average. The bagging process, by averaging predictions from bootstrap samples, helps reduce variance and mitigates overfitting issues in the model. As shown in Figure S1, the entire data set is randomly divided into two groups, one is the training data set, used to build the random forest model; the other is the test data set, used for testing without seeing the data set. The training data set accounts for 70% of the total data, and the rest is test data. Grange et al. (2018) built the RF model using the R "normalweather" package.

In our study, the parameters of the RF model are as follows: hourly concentrations of HONO, NO, NO_2, O_3, $PM_{2.5}$, SO_2, and CO as dependent variables, meteorological parameters (wind direction, wind speed, air temperature, humidity, and atmospheric pressure) and Time predictors (weekdays, hours) served as independent predictors. The training set uses randomly selected 70% of the data, and the remaining 30% is used as the test set. Random forest models were developed using the rmweather R package (Grange et al., 2018; Grange and Carslaw, 2019). The number of trees is 300, and the number of variables split in each node is 3. For each weather normalization, the explanatory variables are resampled (excluding the time variable) without replacement and randomly assigned to the dependent variable observations. The 1000 predicted values are then aggregated using the arithmetic mean to obtain the deweathered concentration.

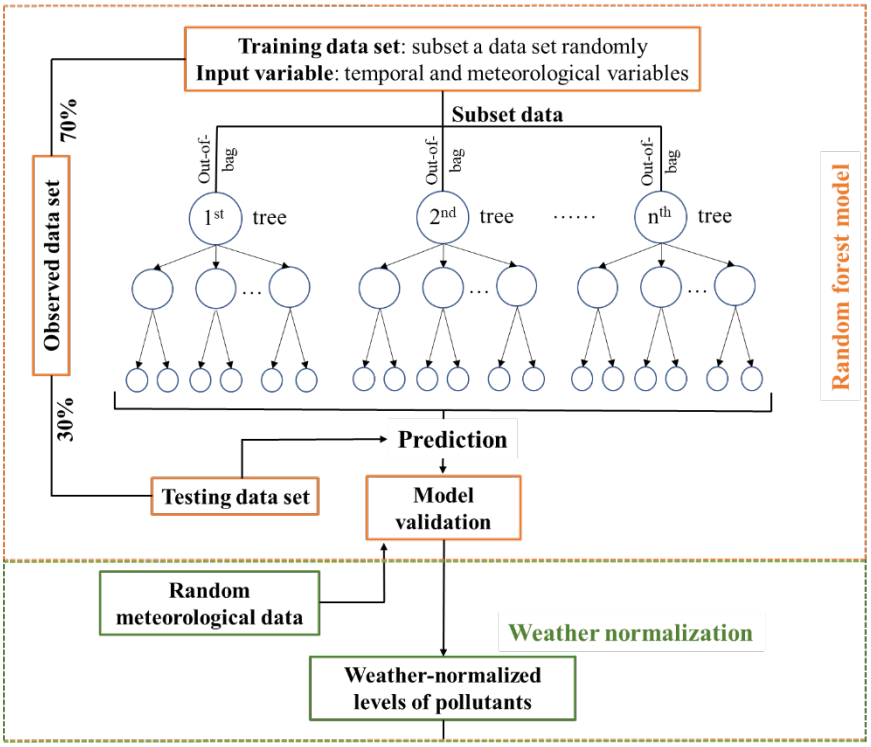

Fig. S1. The flowchart of the machine learning based RF algorithm.

Model performance evaluation

Evaluation metrics for the model can be found in Table S5. The random forest model showed good performance in predicting the data compared to the observations in the training and test datasets. Specifically, the R values range from 0.93-0.98. These extremely high correlation values indicate a strong relationship between the predicted values and the observed values, indicating that the characteristics of the established model are excellent. The FAC2 of each indicator is very small, indicating that our model meets the conditions for predicting scores. Likewise, lower NMB and NMGE values indicate that our model performs well. Through the verification of various indicators, it is believed that the model has good prediction ability.

Table S5. RF model performance for testing data set (in hourly time resolution).

Pollutants	RMSE	R	FAC2	MB	MGE	NMB	NMGE
HONO	0.21	0.93	0.86	0.01	0.15	0.02	0.21
NO	7.30	0.93	0.34	-0.21	3.76	-0.03	0.50
NO_2	4.38	0.94	0.93	-0.04	3.12	0.00	0.16

O_3	4.04	0.95	0.84	0.12	2.91	0.01	0.16
SO_2	0.63	0.93	0.68	0.01	0.38	0.01	0.27
CO	164.55	0.96	1.00	4.22	114.60	0.00	0.13
$PM_{2.5}$	12.88	0.98	0.88	0.83	8.70	0.01	0.15

Note: FAC2 (fraction of predictions with a factor of two), MB (mean bias), MGE (mean gross error), NMB (normalized mean bias), NMGE (normalized mean gross error), COE (Coefficient of Efficiency), IOA (Index of Agreement).

In the revised SI, we have added Table S6(Table R2). After deweather, the concentration changes of different pollutants in the two time periods will be introduced in detail in the subsequent replies.

Table R2. Periods and concentration after deweather (mean ± standard deviation) of $PM_{2.5}$, HONO, trace gases in field observation, and the percentages in parentheses are concentration changes after deweather. Relative change in observed values and deweather values in different periods.

Category	BCNY (1.1-1.24)		COVID (1.25-3.6)		Relative change	
	Deweather	Observed	Deweather	Observed	Deweather	Observed
$PM_{2.5}$ ($\mu g/m^3$)	45.22±28.56 (-4.26%)	47.23±44.50	67.92±57.97 (-2.28%)	69.86±67.26	+50.20%	+47.91%
HONO (ppb)	0.89±0.37 (-8.25%)	0.97±0.74	0.51±0.25 (-3.77%)	0.53±0.45	-42.70%	-45.36%
NO (ppb)	15.44±18.40 (-16.18%)	18.42±29.24	3.24±2.05 (+32.79%)	2.44±5.40	-79.02%	-86.75%
NO_2 (ppb)	23.28±7.28 (-13.75%)	26.99±13.41	16.43±5.98 (-4.81%)	17.26±11.34	-29.42%	-36.05%
CO (ppb)	823.60±318.92 (-9.27%)	907.72±499.16	896±488.29 (-6.17%)	954.87±624.04	+8.79%	+5.19%
SO_2 (ppb)	2.27±0.69 (+8.61%)	2.09±1.36	1.48±1.18 (+0.68%)	1.47±1.95	-34.80%	+29.67%
O_3 (ppb)	16.98±5.62 (+39.64%)	12.16±10.79	22.60±4.10 (+6.15%)	21.29±11.78	+33.10%	+75.08%

2. Chemical lifetimes. The paper in effect performs a steady state analysis on HONO,

assuming any rate of change of concentration can be related to an imbalance in the in-situ source and sink terms. You can do this for short-lived species – such as OH – but only with care for species such as HONO, with lifetimes (these are midlatitude winter measurements) of tens of minutes. The measured HONO reflects the integrated chemical variability over the sampled airmass trajectory prior to its arrival at the measurement point. This will be heterogeneous – especially at ground level in the middle of a city (i.e. the OH and NO_2, etc will have varied a lot over the period of time – given by the HONO lifetime – that the airmass has traveled to the measurement point within the city). See arguments developed by Lee et al, JGR 2013, and related papers.

Response: Thank you for your good comments and suggestions. We agree with you that the measured HONO reflects the integrated chemical variability over the sampled airmass trajectory prior to its arrival at the measurement point. This might introduce uncertainty about the budget analysis using a steady state analysis. To confirm the possible affected areas, we carefully checked the representativeness of the dataset. Firstly, a potential source contribution function (PSCF) of HONO has been analyzed. Given a 10 min lifetime of HONO, the spatial distribution of HONO in the P2 is highly similar to that when compared with that in the P1 as shown in Figure R2. This means air mass should have a similar impact on the HONO budget during these two periods. Secondly, we carried out deweather analysis using a random forest algorithm combined with a machine learning model. The details are shown in the SI. We found meteorology has little influence on HONO concentration during the whole observation period. This means HONO concentration is dominated by primary emissions and secondary formation. Thirdly, we compared the concentrations of HONO at BUCT and Institute of Atmospheric Physics (IAP) from Jan. 5th to Mar 24th when the data are available (Figure R3). The linear distance between these two sites is ~8 km. The HONO concentrations are comparable at these two sites. Thus, even though the concentration changes represent the integrated chemical variability over the sampled airmass trajectory prior to its arrival at the measurement point, it still represents the local feature in urban Beijing. Finally, the instrumentation time resolution of LOPAP was 6 s. We calculated the variation coefficient for the datasets with different time resolution, i.e., 1

h *vs* 6 s. A small variation coefficient of ~0.02-0.05 implies that a small uncertainty of HONO budget might be resulted from the lifetime of HONO. Thus, we think the possible uncertainty should not have a large influence on our conclusions when the budget is compared at a fixed site between two different periods.

In lines 206-215 in the revised manuscript, we added a short paragraph to clarify this possible uncertainty as "Given that the result of potential source contribution function (PSCF, Fig S2), the source distribution of HONO between BCNY and COVID was highly similar and the trend of HONO was similar (Pearson'r=0.78) between BUCT and Institute of Atmospheric Physics (IAP, 8 km away from BUCT), the steady state analysis on HONO is appliable and reasonable even though the lifetime of HONO is several minutes in the atmosphere. In addition, the instrumentation time resolution of LOPAP was 6 s. We calculated the variation coefficient for the datasets with different time resolutions, i.e., 1 h *vs* 6 s. A small variation coefficient of ~0.02-0.05 implies that a small uncertainty of the HONO budget might result from the lifetime of HONO. Thus, we think the possible uncertainty should not have a large influence on our conclusions when the budget is compared at a fixed site between two different periods". And we have added Figure R2 as Figure S2 in the revised SI.

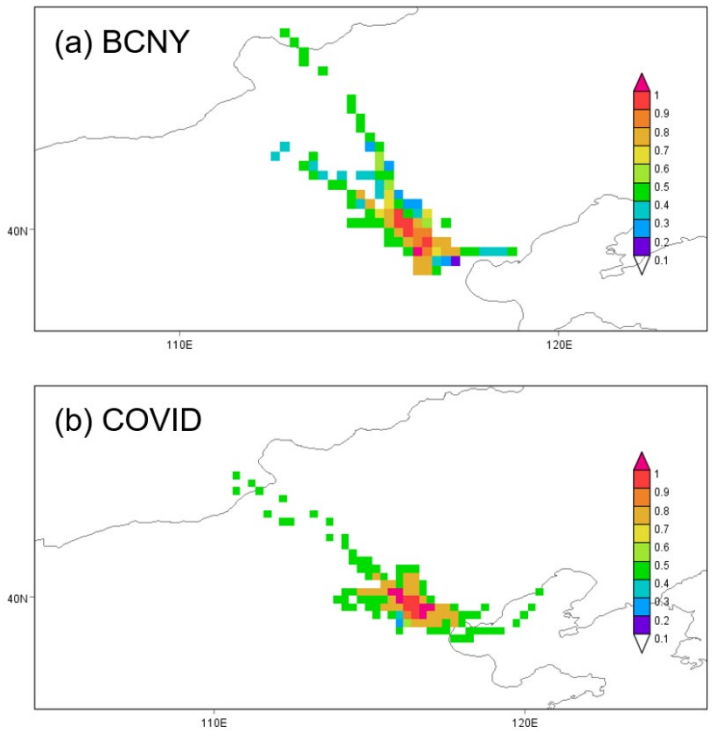

Figure R2. The potential source contribution function (PSCF) maps for the concentration of HONO (a and b are BCNY and COVID, respectively). The trajectory of the air mass is 12 hours.

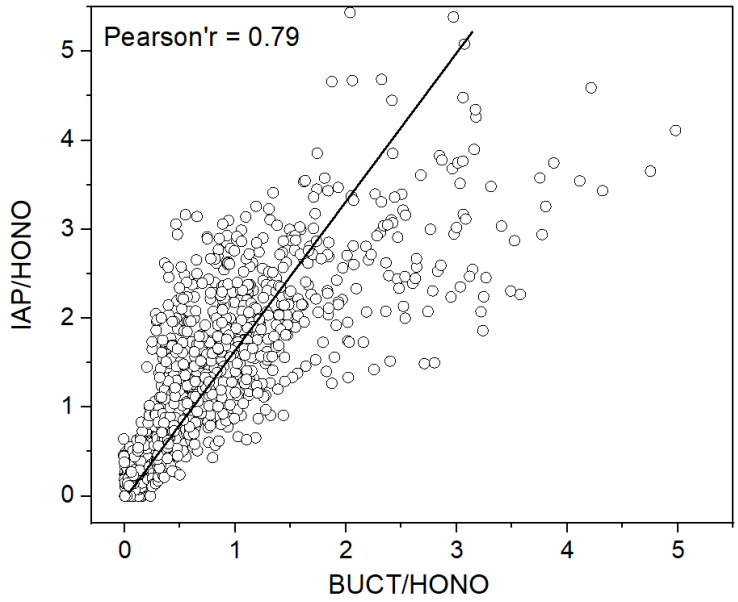

Figure R3. The comparison of HONO concentration between IAP and BUCT from Jan. 5th to Mar 24th.

3. Statistical significance/precision/uncertainty. The paper does not consider sufficiently the uncertainty in the (many) source and sink terms considered, and their propagation together (beyond the Monte Carlo result, which I can't believe includes the uncertainty in the individual inputs, e.g. OH concentrations). Is there any statistical power resulting from their combined uncertainties? Are the uncertainties given in the paper 1 or 2 standard deviations? Are differences statistically significant? The ± ranges – even assuming these are 1 sd – suggest not (e.g. HONO/NO_2 ratio – changing from 0.038 ± 0.035 to 0.042 ± 0.034 – this is not a meaningful (statistically significant) change). There are several examples.

Response: Thank you for your comments and suggestions. As for your questions, we will reply one by one.

In our calculation, ten key parameters including source terms and sink terms were considered, and their respective fluctuation ranges were input, and then Monte Carlo was used to calculate the respective sensitivity distributions and uncertainties. In

addition, through comparison with field observations in the Beijing area, we found that our OH fitting performance is good. Of course, it should be noted that when the fluctuation range of various parameters were input, this may still bring some deviations although we have given full consideration and optimized based on existing research. Considering that the sources and sinks of HONO are complex and the selection of parameters in different studies may even differ by several orders of magnitude, our results should generally perform well.

For the comprehensive uncertainty, the uncertainty given in the paper is 1 standard deviation. In the revised manuscript, we added a description where it first appears "During P1, the measured concentration of $PM_{2.5}$ varied between 0.2-288 μg m^{-3} and the mean concentration was 47.2 ± 44.5 (mean ± 1σ) μg m^{-3}." in lines 318-319. And we added the sentence "The relative standard deviation is 27.2% for the HONO budget (details are in SI)" in line 624. In the revised SI, we added an introduction to the Monte Carlo algorithm. The added content is as follows:

Text S2 Monte Carlo algorithm

The Monte Carlo algorithm is a method of estimating numerical values through random sampling. It can be used to estimate the overall uncertainty of the numerical value. A large number of samples are generated by random sampling from a probability distribution and the required numerical indicators are calculated based on these samples. Due to the limited number of samples, there is a certain error between the estimated value and the true value. We increase the number of sampling times to 10,000 to reduce statistical uncertainty.

When establishing the simulation model, the respective change ranges of the variables that affect HONO intensity are input, and the uncertainty of the modeling is evaluated by sampling from the probability distribution of the parameters to obtain the overall uncertainty. In addition, the uncertainty of the model parameters is propagated to the model output through Monte Carlo sampling, and the uncertainty distribution of the results can be obtained. The formula for overall uncertainty can be expressed as:

$$\sigma = \sqrt{\frac{1}{N}\sum_{i=1}^{N}(x_i - \bar{x})^2}$$

σ represents the standard deviation of the overall uncertainty; N is the number of samples; x_i is the value of the i-th sample, and $\bar{x}$ is the mean of the sample.

T-tests have been performed to confirm the significance of the differences mentioned in the manuscript and to the differences are statistically significant. For the ± range that exists in the manuscript, such as "The HONO/NO_2 in the P2 period was higher than that in the P1 stage, especially in the daytime, although the values of HONO/NO_2 in both stages (P1: 0.036 ± 0.016; P2: 0.041 ± 0.038) were lower than that (0.052-0.080) reported by Cui et al (Cui et al., 2018). Subsequently, we further analyzed $HONO_{corr}/NO_2$ (details shown in Sect. 2.2). The $HONO_{corr}/NO_2$ attributed to secondary formation via heterogeneous reactions changed obviously after subtracting the interference of other HONO sources. As shown in Fig. S5, the daytime peak of $HONO_{corr}/NO_2$ in P2 became more prominent compared with that in Fig. 3e. At the same time, the $HONO_{corr}/NO_2$ (0.038 ± 0.035) in P1 was slightly lower than that in P2 (0.042 ± 0.034)" in the lines 471-479 of the manuscript, it's still a statistically significant change at 0.05 level according to the T-test result.

Minor comments

I've noted some more points below but the authors need to address the points noted above vs the overall approach, to have confidence that the results of their analysis allow them to draw the conclusions presented in the paper.

1. Introduction – reviews different sources for HONO and their contribution, but this mixes together very different environments (i.e. the relative importance of different sources will vary for the measurement site vs a road tunnel vs a bare soil location vs the marine boundary layer vs livestock). Suggest distilling this to assess the key factors at the measurement location, ie city center.

Response: Thank you for your good suggestion. In lines 67-135 in the revised manuscript, we revised the description as you suggested.

In the revised SI, we have added Table R2 as Table S1 and updated the sentence "The sources of atmospheric HONO consist of direct emissions and secondary

formation in the atmosphere. Direct emissions include soils, biomass burning, vehicles, indoor air, and livestock farming. Soil emissions, which depend on soil types, microorganisms, water content, temperature, and pH (Kulmala and Petäjä, 2011; Weber et al., 2015; Kim and Or, 2019), are important sources of HONO. Biomass burning, often occurs in the summer and autumn when wheat/corn is harvested and wildfires are common (Zhang et al., 2019b; Sun et al., 2017; Sun et al., 2018; Peng et al., 2020). Vehicle emissions are considered an important source of HONO in traffic-intensive areas (Kramer et al., 2020; Li et al., 2021a). This source is more important at nighttime compared with daytime (Zhang et al., 2016; Fu et al., 2019; Liu et al., 2020c). Recently, indoor emissions have also been proposed as a potential HONO source (Xue, 2022), which is related to the ventilation from high HONO concentrations in indoor air to low HONO concentrations in outdoor air (Zhang et al., 2019b). Livestock farming is a previously overlooked source of HONO, especially in agricultural areas.

Secondary formation of HONO includes gas-phase reaction between NO and OH radicals, photolysis of particulate nitrate, and heterogeneous reaction of NO_2 on ground and particulate matter surfaces, including photochemical heterogeneous reaction of NO_2. Gas phase reaction between NO and OH, photolysis of nitrate particles, and light-enhanced conversion of NO_2 are the main daytime sources of HONO (Liu et al., 2019b; Liu et al., 2020c; Zhang et al., 2022). Furthermore, acid replacement processes may be a non-negligible source of daytime HONO in locations affected by soil-borne mineral dust deposition (Vandenboer et al., 2014). The heterogeneous reaction of NO_2 on various surfaces is widely regarded as an important source of HONO (Han et al., 2016; Liu et al., 2020a).

We summarized the sources of HONO and the locations of observation sites in the literature (Table S1). The type of observation site often has a great impact on the source intensity and contribution proportion of each source of HONO. In natural ecological areas or Antarctic stations with little human activity, the photolysis of nitrate is the main source of HONO during the day, and its contribution is much higher than the homogeneous reaction of NO and OH (Bond et al., 2023; Tang et al., 2024). In the ocean or areas close to the sea, the heterogeneous transformation of NO_2 becomes the

main source of HONO, and the transformation on the aerosol surface may be more important than that on the ground (Xing et al., 2023). In smoke collected near wildfires, it was found that the heterogeneous conversion contribution of NO_2 can reach 85%, making it the most important source of HONO (Chai et al., 2021). Emissions from soil and biological soil crusts are important in some areas where vegetation and soil are exposed (Meusel et al., 2018). For three different types of observation sites: rural, suburban, and urban, the relative importance of sources is also obviously different. In rural areas, there are usually no traffic activities, and are mainly affected by agricultural activities and animal husbandry, so traffic emissions can be ignored. During periods of intensive agricultural activity, soil emissions are the main source of HONO, accounting for up to 80% (Liu et al., 2019b). When there is little agricultural activity, the reaction of NO and OH and the heterogeneous transformation of NO_2 on the ground become the two main sources in rural areas (Xue et al., 2020; Song et al., 2022), accounting for up to 70%. In rural areas with developed animal husbandry, its direct emissions can contribute 39-45% of HONO (Zhang et al., 2023). Suburbs are mostly covered by vegetation, with a small number of villages nearby. The heterogeneous conversion of NO_2 is the main source of HONO, which can reach 70% of HONO sources (Fu et al., 2019; Ye et al., 2023). For highways, tunnels, and urban areas with heavy traffic, traffic emissions usually dominate HONO sources, accounting for 40% to 80% of HONO sources (Xu et al., 2015; Zhang et al., 2019c; Liu et al., 2020c; Kramer et al., 2020). In some ordinary urban areas where traffic activities are not so intensive, the heterogeneous conversion of NO_2 and the reaction of NO and OH are also the main sources of HONO in addition to traffic sources. It can be seen that the relative importance of different sources is often affected by the type of emission source near the observation site.

Although intensive studies have been performed on HONO sources, the contributions of different sources are still controversial (Zhou et al., 2011; Liu et al., 2014; Wu et al., 2019; Kramer et al., 2020; Meng et al., 2020). For the same type of observation area, the contribution of each source still diverges in different studies. For example, in mixed residential, commercial, and traffic areas, the importance of traffic

emissions varies greatly. In some studies, it accounts for as much as 50% (Liu et al., 2020c; Zhang et al., 2019a; Tong et al., 2016), while in some studies, it can be ignored (Zhang et al., 2020). A similar situation exists for the heterogeneous conversion of NO_2. Some studies suggest that this process is not important (Tong et al., 2015; Zhang et al., 2019c; Zhang et al., 2022), while some studies believe that it can contribute at least 70% of HONO (Meng et al., 2020; Zhang et al., 2020; Jia et al., 2020). It should be noted that the contribution of NO_2 heterogeneous reaction to HONO greatly depends on the choice of NO_2 uptake coefficient (γ_{NO2}), which varies from 10^{-8} to 10^{-4} in different studies (Meng et al., 2020; Liu et al., 2020a; Ge et al., 2019; Liu et al., 2015; Liu et al., 2020c). Vehicle emissions also have similar characteristics because the HONO emission rate strongly depends on the emission factor, i.e. the ratio of $HONO/NO_x$ (Kramer et al., 2020; R. Kurtenbach et al., 2001; Zhang et al., 2019c), which ranges from 0.03% to 2.1% (Liao et al., 2021). For other HONO sources, the relative importance is affected by many parameters, such as reaction kinetics for photolysis of nitrate, OH concentrations for homogeneous reaction between NO and OH, emission fluxes for soil emissions, and so on. Thus, the HONO budget still has a large uncertainty. In particular, it is an open question of how to prove the importance of a specific reaction pathway or a source of atmospheric HONO."

Table R2. Summary of HONO observation sites and source contributions

Location (References)	Date	Measurement area	Site situation	Source contribution
Antarctica (Bond et al., 2023)	2022.01	Research Station	Clean area, covered with ice and snow	Photolysis of nitrate in snow is very important, and its contribution is 10 times greater than the reaction between NO and OH.
Shenzhen (Tang et al., 2024)	2019.10	natural ecological area	Along the coast, there are fewer human activities and more vegetation.	Photolysis of large amounts of nitrate in coarse particles completely compensates for unknown sources during the daytime (66%).
China (Xing et al., 2023)	2018.05	sea edge	coastal	In inland areas, the NO_2 heterogeneous reaction on the ground is more important; in coastal and ocean cases, the contribution of aerosol surfaces is greater.
Idaho (Chai et al., 2021)	2018.08	wildfire zone	Smoke collected near five wildfires	In the aging smoke during the daytime, the heterogeneous conversion of NO_2 reaches 85%, followed by NO+OH.
Guangzhou (Li et al., 2012)	2006.07	rural area	Close to farmland, low traffic emissions	The main source at night is NO+OH and the heterogeneous conversion of NO_2 on the ground, and traffic can be ignored
Cyprus (Meusel et al., 2018)	2016.04	rural area	Along the coast, a lot of vegetation is exposed	Emissions from soil and biological soil crusts are important.
Melpitz (Ren et al., 2020)	2018.04	rural area	Nearby are meadows, agricultural areas, and forests	Nocturnal HONO: Heterogeneous conversion of ground NO_2 dominates, and traffic emission is a secondary source.
Wangdu (Liu et al., 2019b)	2014.06	rural area	Intensive agricultural activities and no traffic emissions	Noonday HONO: Soil emissions account for 80%.
Wangdu	2017.12	rural area	No traffic emissions,	Noonday HONO: The heterogeneous conversion of NO_2 on

(Xue et al., 2020)			surrounded by farmland	the ground is 36%, NO+OH is 34%, and the others can be ignored.
Wangdu (Song et al., 2022)	2020.06-2020.09	rural area	No traffic emissions, surrounded by farmland	Noonday HONO: The heterogeneous conversion of NO_2 on the ground is dominant (43-62%), followed by NO+OH 12-38%, and the rest are less than 5%.
Wangdu (Zhang et al., 2023)	2020.09-2021.08	rural area	Seriously affected by agriculture and animal husbandry	Direct emissions from rural areas, including animal husbandry, account for 39-45% and cannot be ignored.
Hongkong (Zhang et al., 2016)	2011.08	suburbs	Near the airport, surrounded by vegetation and close to the South China Sea	The heterogeneous conversion of NO_2 on the ground is 42%, soil emission is 29%, marine source is 9%, NO+OH is 6%, aerosol surface conversion is 3%, and traffic is 2%.
Hongkong (Xu et al., 2015)	2011.08-2012.05	suburbs	Areas near airports and highways are mostly covered by vegetation.	Nocturnal HONO: Traffic dominates in the first half of the night (59%), and the heterogeneous conversion of NO_2 on the ground dominates in the second half of the night.
Heshan (Fu et al., 2019)	2017.01	suburbs	Lots of vegetation and farmland, with some scattered villages	Heterogeneous conversion of NO_2 is 72%, traffic is 8%, and NO+OH is 3%. Noonday HONO: Photolysis of nitrate accounts for more than 50%.
Taizhou (Ye et al., 2023)	2018.06	suburbs	Borders farmland and fish ponds	Noonday HONO: The heterogeneous conversion of NO_2 on the ground is 71%, followed by NO+OH, traffic, and aerosol surface conversion. Nocturnal HONO: Heterogeneous conversion of NO_2 on the ground is dominant (55%).
Beijing (Tong et al., 2015)	2014.11	urban area	Densely populated and busy with traffic	Nocturnal HONO: Traffic emission is 40%, NO+OH is 42%, and others are 18%.
		suburbs	By the lake, with farmland	Nocturnal HONO: Traffic emission is 8%, NO+OH is 11%,

			nearby	and others are 81%。
Beijing (Tong et al., 2016)	2014.12	urban area	Densely populated and busy with traffic	Nocturnal HONO: Traffic emission is dominant (49%), and the reaction of NO and OH is also important.
		suburbs	By the lake, with farmland nearby	Nocturnal HONO: Heterogeneous conversion of NO_2 is the main source, and traffic is 10%.
Beijing (Zhang et al., 2019a)	2006.08	urban area	Mixed residential, commercial, and transportation area	Nocturnal HONO: Traffic is 41%, ground heterogeneous conversion is 27%, and aerosol surface conversion is 20%. Noonday HONO: ground heterogeneous conversion is 66%, and aerosol surface conversion is 19%.
Beijing (Zhang et al., 2019c)	2016.12	urban area	Densely populated and busy with traffic	Nocturnal HONO: Traffic emission is dominant, reaching 52%, and heterogeneous conversion is not an important pathway.
Beijing (Meng et al., 2020)	2016.12	urban area	Mixed residential, commercial, and transportation area, 325m vertical observation.	High altitude during haze: HONO is dominated by heterogeneous conversion on the aerosol surface; Near the ground: Heterogeneous conversion of NO_2 on the ground is dominant, followed by traffic, accounting for 29%
Beijing (Gu et al., 2021)	2017.05 2018.01	urban area	Mixed residential, commercial, and transportation area	Noonday HONO: The light-induced heterogeneous transformation of NO_2 on the ground is dominant, and aerosol surface conversion can be ignored. Noonday HONO: NO+OH is dominant.
Beijing (Liu et al., 2020c)	2018.02-2018.07	urban area	Mixed residential, commercial, and transportation area	Nocturnal HONO: Traffic emission is dominant, reaching 50%, and heterogeneous conversion is not an important pathway. Noonday HONO: Nitrate photolysis and NO+OH are important.

Beijing (Zhang et al., 2020)	2018.04	urban area	Mixed residential, commercial, and transportation area, 325m vertical observation.	At different altitudes, the heterogeneous conversion of NO_2 is the most important source, accounting for more than 70%. Among them, the aerosol surface is dominant.
Beijing (Jia et al., 2020)	2018.08	urban area	Mixed residential, commercial, and transportation area	Traffic is 18%, NO+OH is 31% (clean) and 7% (haze), and the aerosol surface conversion can reach up to 88%, which is very low on the ground. Nitrate photolysis is 15%,
Beijing (Liu et al., 2021)	2018.06 2018.12	urban area	Mixed residential, commercial, and transportation area	Noonday HONO: NO+OH is 22%, traffic is 19%, and Heterogeneous conversion on the aerosol surface is 19%。 Noonday HONO: Heterogeneous conversion on the aerosol surface is 30%, Heterogeneous conversion on the ground is 25%, and traffic is 20%.
Beijing (Zhang et al., 2022)	2019.01	urban area	Densely populated and busy with traffic	Traffic is 28%, Heterogeneous conversion on the ground is 27%, and aerosol surface conversion is 15%。
Beijing (Li et al., 2021b)	2019.06	urban area	Mixed residential, commercial, and transportation area	Nocturnal HONO: The heterogeneous conversion of NO_2 is the main pathway, followed by NO+OH. Traffic is 30%.
Shijiazhuang (Liu et al., 2020b)	2019.12-2020.03	urban area	mixed traffic and residential area	Nocturnal HONO: The heterogeneous conversion of NO_2 on the ground is dominant, followed by aerosol surface conversion.
Beijing-Tianjin-Hebei (Zhang et al., 2019b)	2017.12	urban area	Less traffic emissions and intensive agricultural activities	Nocturnal HONO: Traffic and heterogeneous conversion of NO_2 are the main sources.
Xi'an	2015.08	urban area	Mixed residential, commercial,	Nocturnal HONO: The heterogeneous conversion of NO_2 is

(Huang et al., 2017)			and transportation area	the main pathway, followed by NO+OH. Traffic is 19%.
Shanghai (Cui et al., 2018)	2016.05	urban area	Mixed residential, commercial, and transportation area	Nocturnal HONO: Heterogeneous conversion of NO_2 is the main source.
Nanjing (Zheng et al., 2020)	2015.12	urban area	To the west of the steel plant and petrochemical refinery, 15 kilometers from the city center	The heterogeneous conversion of NO_2 is dominant, accounting for 50%, and traffic is 11%.
Nanjing (Liu et al., 2019a)	2017.11-2018.11	urban area	Mixed residential, commercial, and transportation area	Traffic is 23%, heterogeneous conversion on the ground is 36%, Soil emissions can reach 40% in July and August. The aerosol surface conversion reaches 40% (severe haze periods).
Changzhou (Shi et al., 2020)	2017.04	urban area	Mainly residential and commercial areas, with no roads and industrial activities,	Nocturnal HONO: Heterogeneous conversion of NO_2 is 54%, traffic is 32%, and NO+OH is 14%. Noonday HONO: Nitrate photolysis is important.
Guangzhou (Yu et al., 2022)	2018.10	urban area	mixed traffic and residential area	Nocturnal HONO: The three main sources are the heterogeneous conversion of NO_2 on the ground, traffic, and NO+OH. The aerosol surface conversion and soil emissions are not important.
Birmingham (Kramer et al., 2020)	2016.11	urban area	road tunnel	Traffic is dominant, accounting for 66% (up to 86%), the heterogeneous conversion of NO_2 is only 5%,

2. L174 – NO_2 measured by 42i – selectivity for NO_2, the NO_2 data will include other NOy species (including HONO).

Response: Thank you for your good comments. This is taken into account in our observations, so in the calculations, the NO_2 concentration has been subtracted from the HONO concentration. In lines 174-175 in the revised manuscript, we added a sentence "Notably, the NO_2 measured by 42i includes HONO. Thus, it has been corrected".

3. L257 how was $j_{(HONO)}$ calculated

Response: Thank you for your comments. $j_{(HONO)}$ is simulated in MCM using $j_{(NO2)}$ data observed at our site. The details are as follows: In each case, variation of photolysis rate with solar zenith angle can be described well by an expression of the following form,

$$J = l\,(\cos\chi)^m \exp(-n.\sec\chi)$$

by optimizing the values of the three parameters, l, m, and n are the parameters of the reaction respectively, χ is *the* solar zenith angle (Saunders et al., 2003). In line 257 in the revised manuscript, we added a sentence "J_{HONO} is simulated in a box model using J_{NO2} data observed at our site".

4. L190 heterogeneous reactions of NO_2 have been accounted for – I didn't follow this section, may need rewording.

Response: Thank you for your suggestion. I am sorry for confusing you. In the revised manuscript, we made changes and deleted the "have been accounted for" in "The sources including vehicle emissions ($E_{vehicle}$), soil emissions (E_{soil}), the reaction of NO and OH (P_{NO-OH}), the photolysis of particulate nitrate ($P_{nitrate}$), and the heterogeneous reaction of NO_2 ($P_{aerosol}$ and P_{ground})" in lines 190-192.

5. L218 what is the conversion factor alpha?

Response: Thank you for your good suggestion. It is a unit conversion factor of emission flux from g m^{-3} s^{-1} to ppb h^{-1}. In lines 218-219 in the revised manuscript, we update the "conversion factor (α, from g m^{-3} s^{-1} to ppb h^{-1})".

6. L227 using NO_2 and CO – NO_2 concentrations will vary with a lifetime of a minute

or so (with respect to the NOx-O_3 PSS) and 6-12 hours our so (with respect to NOx removal). CO concentrations will vary with a lifetime of several weeks. Is it valid to use both in the same in situ emission analysis?

Response: Thank you for your good suggestion. When calculating k_{het}, equation 3 does not consider the impact of the boundary layer on the concentration of pollutants. CO is considered to be a relatively stable substance and is usually used for partially eliminating the variation of the boundary layer height. Thus, equation 4 corrects the boundary layer variation by normalizing to CO concentration. This method has been widely used to calculate the heterogeneous uptake kinetic of NO_2 on aerosol in previous studies (Zhang et al., 2020; Zhang et al., 2019c; Li et al., 2012). It is expected to get a more accurate k_{het} because the influence of the variation of boundary layer height has been accounted for. It is worth noting that during a year of HONO observations in coastal cities in southeastern China (Hu et al., 2022), the author compared the results of balancing NO_2, CO, and BC and found that CO performed well, and finally selected CO as the parameter for k_{het} calculation.

In lines 233-235 in the revised manuscript, we have pointed out that "To decrease the contribution of boundary layer height variation on the k_{het} calculations, we normalized HONO concentration to CO concentration as the same as reported in the literature (Zhang et al., 2019c; Li et al., 2012)".

7. L257 / table 1 – what is the estimated OH concentration & how does it compare with measurements – the values in L436 (presumably 24 hour mean, around 4-7e5) seem much lower than those observed in wintertime Beijing (2.7e6 as 24-hour mean; Slater et al., 2020).

Response: Thank you for your good suggestion. The article by Slater et al. in 2020 describes it as follows: "Averaged over the full observation period, the mean daytime peak in radicals was 2.7×10^6, 0.39×10^8, and 0.88×10^8 cm^{-3} for OH, HO_2, and total RO_2, respectively". Our estimated 24-hour mean concentration of OH ranges from 1.1×10^5 to 2.5×10^6, which is very close to the daytime peak observed in Beijing in winter (2.7×10^6) (Slater et al., 2020). The daily mean value ($4\text{-}7\times10^5$) is therefore lower than the maximum value at noon. As shown in Figure R4 or S3, the estimated OH concentrations are in good agreement with the observations in Beijing.

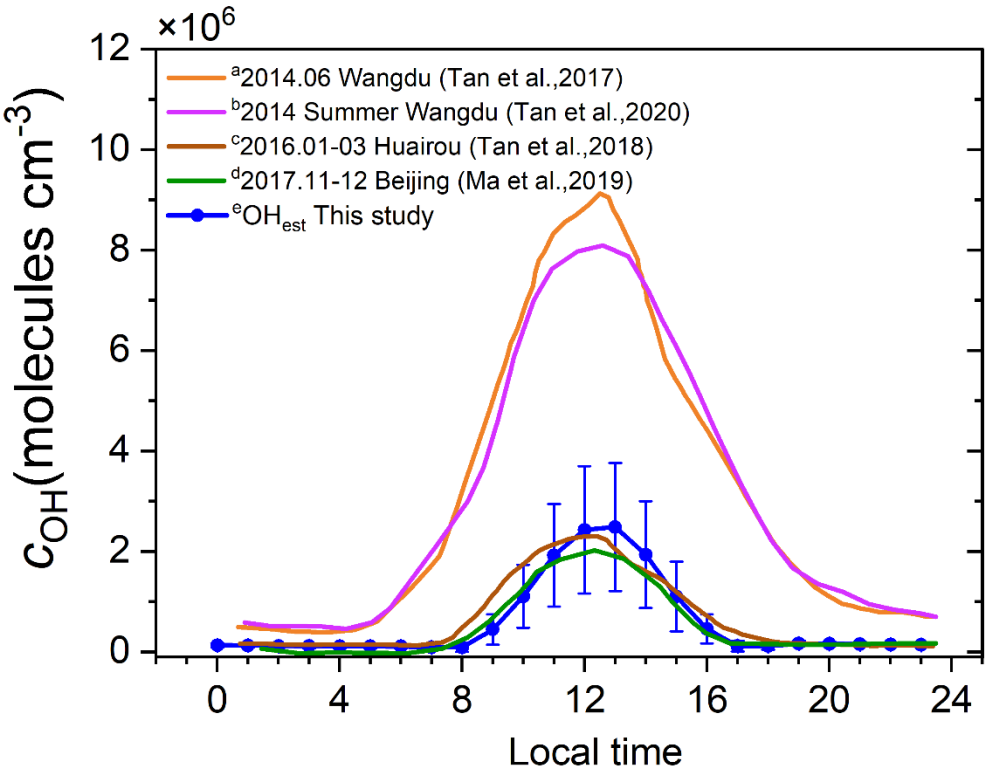

Figure R4. Diurnal variation of OH concentrations observed in different areas of the North China Plain (a-d) (Tan et al., 2017; Tan et al., 2018; Ma et al., 2019; Tan et al., 2020) and parameterized fitting in this study (e).

8. L270 Parameterisation of OH concentrations. We might expect that the main source of OH in Beijing is HO_2 + NO, the main sink for OH is OH + NO, and the main primary source of OH is HONO photolysis (one can then argue about if HONO is acting as a primary source or a reservoir). The parameterization given was developed for rural sites (as the authors note), where NO levels would be much lower, and was developed prior to more recent understanding of HONO abundance (it is over 20 years old). Is it valid to use? L286 – considering these above I do not agree that we can be optimistic about the estimated OH concentrations.

Response: Thank you for your good suggestion. Notably, this parameterization scheme was developed based on measurements at rural sites (Ehhalt and Rohrer, 2000), where NOx concentrations were lower than in urban environments. Alicke et al. (Alicke, 2002) found OH concentrations estimated with this scheme were in good agreement with those calculated according to a pseudo-steady state method during the pollution period in urban environments (such as Milan) although some uncertainty was expected.

In our previous study (Liu et al., 2020d), we also found that the estimated OH concentrations using this method were comparable with those observed values in the North China Plain (Tan et al., 2019). Thus, daytime OH concentrations estimated using this method should be overall credible although the uncertainty is inevitable. Fig R2 (Fig S2) summarizes the observed OH concentrations in the North China Plain. The results estimated in this study are slightly lower than those observed in Wangdu, but almost consistent with those in Beijing and Huairou. In summary, although the parameterization was developed many years ago, judging from the performance results, it still has excellent performance in fitting OH.

In lines 284-287 in the revised manuscript, we have highlighted the points "The results estimated in this study are slightly lower than those observed in Wangdu (Rural), but almost consistent with those in Beijing (Urban) and Huairou (Suburb). In summary, we should be optimistic about the estimation of OH concentration."

9. L370 – $PM_{2.5}$ components increased obviously in P2 vs P1 – from the plot it is not obvious to me that they do: is there a statistically significant change? What about changes in the meteorology?

Response: Thank you for your comment. The increasing trend in Figure 1 is not very obvious, and we further summarize their concentrations in P1 and P2 in Table S4. In the revised manuscript, we added the sentence "It can be seen from Figure 1 and Table S4 in SI. All the major components of $PM_{2.5}$, including sulfate, nitrate, ammonium, chloride, and organic aerosol, increased obviously in P2 compared to P1." in lines 370-372. The difference in $PM_{2.5}$ between the two periods is statistically significant ($P<0.05$). In the revised manuscript, we added the sentence "The $PM_{2.5}$ concentration after deweather increased significantly from 45.22±28.56 in P1 to 67.92±57.97 μg m^{-3} in P2 at a confidence level of 0.05, with an increase of 50.2%." in lines 353-355.

10. L410 the traffic index data are useful. Consider showing P1/P2 on these plots. Consider changing the box/whisker plot to linear (not log) – this will assist the reader to follow which differences are statistically significant.

Response: Thank you for your good comment. We have changed the logarithmic plot of Figure 2b into a linear plot.

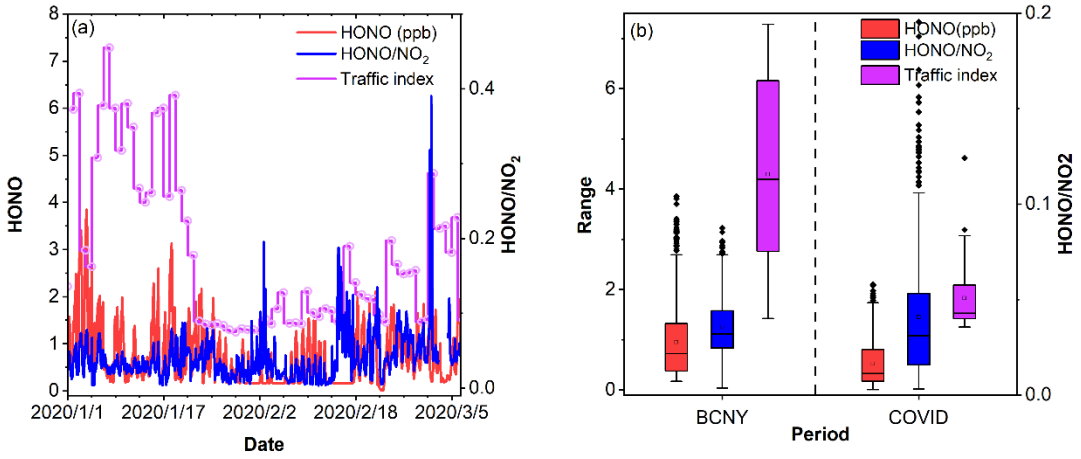

Figure R2. (**a**) Times series of HONO, traffic index, and HONO/NO_2, (**b**) Box plots of HONO, HONO/NO_2, and the traffic index in Beijing during different periods (BCNY=P1, LOCK=P2).

11. concentrations of NO changed: You cannot conclude this without a statistical test, esp for NO_2 and HONO.

Response: Thanks for your suggestion. Regarding the decrease in NO concentration, we did a T-test and found that there was a significant difference in the concentrations between the two time periods ($P<0.05$). In lines 588-589, it has been pointed out as "This can be explained by the significant decrease ($P < 0.05$) in NO and direct emissions of HONO from traffic."

12. L449 Figure 3 the shift in diurnal profiles is interesting, explore further (esp panel 5, HONO/NO_2)?

Response: Thanks for your suggestion. The daily variation curves can provide us with a lot of information. For example, HONO, NOx, SO_2, and O_3 show similar diurnal variations, while the concentrations of HONO, NOx, and SO_2 decrease obviously during the COVID lockdown when compared to that before the COVID lockdown and O_3 concentrations increase. However, the diurnal curves of HONO/NO_2 and $PM_{2.5}$×NO_2 show obvious daytime peaks during the COVID lockdown, which are different from those before the lockdown. In addition, their nocturnal values are comparable between the two periods, while their daytime values are higher during the COVID lockdown than those before the lockdown. Because both HONO/NO_2 and $PM_{2.5}$×NO_2 are indicators for the heterogeneous reaction of NO_2 on aerosols to form HONO, these results imply that the heterogeneous reaction rate during the COVID lockdown should

be higher than that before the lockdown. However, the absolute concentrations of HONO during the COVID lockdown are lower than those before the lockdown. It suggests that heterogeneous reactions should be an unimportant source of HONO in Beijing.

In lines 485-487 in the revised manuscript, we emphasize this point "In summary, we propose that during our observation period, heterogeneous reactions of NO_2 should have a relatively minor contribution to HONO production".

13. L479 contribution (not interference) of other HONO sources. This matters vs literature discussion of interferences in some HONO measurement approaches.

Response: Thanks for your good suggestion. In our $HONO_{corr}$ calculation method, primary and other secondary sources of HONO not attributing to heterogeneous reactions have been subtracted. Thus, the obtained value is more reasonable to present a heterogeneous conversion of NO_2.

To make it clearer, we revised the sentence in lines 478-479 in the revised manuscript as "The $HONO_{corr}/NO_2$ attributed to secondary formation via heterogeneous reactions changed obviously after subtracting other secondary HONO sources".

14. L403 ifs there any info on changes in fleet composition? Big change in total traffic, but the greatest change may be in discretionary journeys (private cars) while deliveries etc(potentially much greater per-vehicle emitters) may have continued.

Response: Thanks for your suggestion. Unfortunately, changes in fleet composition are unavailable. The situation you mentioned may exist, that is, some delivery trucks still have continued. It should be noted that if the HONO emissions by trucks along with the heterogeneous reaction sources increase during the lockdown, an increase in HONO concentrations should be observed. Thus, we ascribe the reduction of HONO concentrations to the decrease in total emissions of HONO from vehicles as supported by the decreases in the traffic index. Therefore, even if the emissions of trucks increase due to the load, this increase is still insignificant compared to the overall emissions of vehicles before the lockdown.

15. L612 the agreement is good to see but is there really confidence in the combined uncertainty of the terms entering the calculation – especially [OH] – to have confidence? L625 same point.

Response: Thanks for your good suggestion. Your opinion is very reasonable. Although we have calibrated each parameter strictly and as accurately as possible, we still cannot guarantee 100% accuracy. For example, for the fitting of OH radicals, although our fitting agrees well with the observations in Beijing, this still does not mean that our results are 100% correct. Considering the complex sources of HONO, uncertainty in the calculation is inevitable, while it is acceptable. In particular, the estimated hourly HONO concentrations are well in agreement with the observed ones. There are 27.2% in total. This means that the simultaneous equations (6 sources and 4 sinks) have been verified 10,000 times. To our best acknowledgment, this is the first time to constrain the parameterization for HONO source budget analysis based on steady-state analysis.

16. L638 plus – these changes must be considered in the context of (potential) changes in meteorology between the two periods – it can be very misleading to simply compare means calculated from two different, fairly short, date periods.

Response: Thanks for your good suggestion. Your suggestion is great. Changes in atmospheric pollutant concentration are affected by emissions and meteorology. The concentrations and relative changes of each pollutant after deweather are recorded in Table R2 (Table S6).

In the revised manuscript, we added the sentence "After removing meteorological factors, the change proportions of $PM_{2.5}$ concentration in the two stages were -4.26% and -2.28% respectively. The HONO changes were -8.25% and -3.77% respectively, the CO changes were -9.27% and -6.17% respectively, and the SO_2 changes were +8.61% and +0.68% respectively. The change proportions are all less than 10%, which means that the impact of changes in meteorological factors on $PM_{2.5}$, HONO, CO, and SO_2 is very weak. However, the change proportions of NO in the two stages were -16.18% and +32.79%, respectively, and O_3 was +39.64% and +6.15% respectively. The change ratio is greater than 30%, indicating that NO and O_3 are greatly affected by meteorology. In addition, the changes in NO_2 were -13.75% and -4.81% respectively, implying that NO_2 is also affected by meteorological factors. From the entire observation period, except for O_3, the changes of other species in the two periods fluctuated between 2.3% and 7.8% after deweather, all less than 8%. In general, after removing the meteorological effects, NO increased by 79%, NO_2 increased by approximately 29%, HONO decreased by approximately 43%, and $PM_{2.5}$ increased by approximately 50%. It is worth noting

that O_3 increased by about 33%, which is much lower than the change in observed values (75.08%) (as shown in Table S6)." lines 639-653.

References:

Bond, A. M. H., Frey, M. M., Kaiser, J., Kleffmann, J., Jones, A. E., and Squires, F. A.: Snowpack nitrate photolysis drives the summertime atmospheric nitrous acid (HONO) budget in coastal Antarctica, Atmospheric Chemistry and Physics, 23, 5533-5550, 10.5194/acp-23-5533-2023, 2023.

Breiman, L.: Random Forests, Machine Learning, 45, 5-32, https://doi.org/10.1023/A:1010933404324 2001.

Chai, J., Dibb, J. E., Anderson, B. E., Bekker, C., Blum, D. E., Heim, E., Jordan, C. E., Joyce, E. E., Kaspari, J. H., Munro, H., Walters, W. W., and Hastings, M. G.: Isotopic evidence for dominant secondary production of HONO in near-ground wildfire plumes, Atmospheric Chemistry and Physics, 21, 13077-13098, 10.5194/acp-21-13077-2021, 2021.

Cui, L., Li, R., Zhang, Y., Meng, Y., Fu, H., and Chen, J.: An observational study of nitrous acid (HONO) in Shanghai, China: The aerosol impact on HONO formation during the haze episodes, Sci Total Environ, 630, 1057-1070, 10.1016/j.scitotenv.2018.02.063, 2018.

Fu, X., Wang, T., Zhang, L., Li, Q., Wang, Z., Xia, M., Yun, H., Wang, W., Yu, C., Yue, D., Zhou, Y., Zheng, J., and Han, R.: The significant contribution of HONO to secondary pollutants during a severe winter pollution event in southern China, Atmospheric Chemistry and Physics, 19, 1-14, 10.5194/acp-19-1-2019, 2019.

Ge, S., Wang, G., Zhang, S., Li, D., Xie, Y., Wu, C., Yuan, Q., Chen, J., and Zhang, H.: Abundant NH3 in China Enhances Atmospheric HONO Production by Promoting the Heterogeneous Reaction of SO2 with NO2, Environ Sci Technol, 53, 14339-14347, 10.1021/acs.est.9b04196, 2019.

Grange, S. K. and Carslaw, D. C.: Using meteorological normalisation to detect interventions in air quality time series, Sci Total Environ, 653, 578-588, 10.1016/j.scitotenv.2018.10.344, 2019.

Grange, S. K., Carslaw, D. C., Lewis, A. C., Boleti, E., and Hueglin, C.: Random forest meteorological normalisation models for Swiss PM_{10} trend analysis, Atmospheric Chemistry and Physics, 18, 6223-6239, 10.5194/acp-18-6223-2018, 2018.

Gu, R., Shen, H., Xue, L., Wang, T., Gao, J., Li, H., Liang, Y., Xia, M., Yu, C., Liu, Y., and Wang, W.: Investigating the sources of atmospheric nitrous acid (HONO) in the megacity of Beijing, China, Science of The Total Environment, 10.1016/j.scitotenv.2021.152270, 2021.

Han, C., Yang, W., Wu, Q., Yang, H., and Xue, X.: Heterogeneous Photochemical Conversion of NO2 to HONO on the Humic Acid Surface under Simulated Sunlight, Environ Sci Technol, 50, 5017-5023, 10.1021/acs.est.5b05101, 2016.

Hu, B., Duan, J., Hong, Y., Xu, L., Li, M., Bian, Y., Qin, M., Fang, W., Xie, P., and Chen, J.: Exploration of the atmospheric chemistry of nitrous acid in a coastal city of southeastern China: results from measurements across four seasons, Atmospheric Chemistry and Physics, 22, 371-393, 10.5194/acp-22-371-2022, 2022.

Huang, R. J., Yang, L., Cao, J., Wang, Q., Tie, X., Ho, K. F., Shen, Z., Zhang, R., Li, G., Zhu, C., Zhang, N., Dai, W., Zhou, J., Liu, S., Chen, Y., Chen, J., and O'Dowd, C. D.: Concentration and sources of atmospheric nitrous acid (HONO) at an urban site in Western China, Sci Total Environ, 593-594, 165-172, 10.1016/j.scitotenv.2017.02.166, 2017.

Jia, C., Tong, S., Zhang, W., Zhang, X., Li, W., Wang, Z., Wang, L., Liu, Z., Hu, B., Zhao, P., and Ge, M.: Pollution characteristics and potential sources of nitrous acid (HONO) in early autumn 2018 of Beijing, Sci Total Environ, 735, 139317, 10.1016/j.scitotenv.2020.139317, 2020.

Kim, M. and Or, D.: Microscale pH variations during drying of soils and desert biocrusts affect HONO and NH3 emissions, Nat Commun, 10, 3944, 10.1038/s41467-019-11956-6, 2019.

Kramer, L. J., Crilley, L. R., Adams, T. J., Ball, S. M., Pope, F. D., and Bloss, W. J.: Nitrous acid (HONO) emissions under real-world driving conditions from vehicles in a UK road tunnel, Atmospheric Chemistry and Physics, 20, 5231-5248, 10.5194/acp-20-5231-2020, 2020.

Kulmala, M. and Petäjä, T.: Soil Nitrites Influence Atmospheric Chemistry, Science 333, 1586-1587, 2011.

Li, S., Song, W., Zhan, H., Zhang, Y., Zhang, X., Li, W., Tong, S., Pei, C., Wang, Y., Chen, Y., Huang, Z., Zhang, R., Zhu, M., Fang, H., Wu, Z., Wang, J., Luo, S., Fu, X., Xiao, S., Huang, X., Zeng, J., Zhang, H., Chen, D., Gligorovski, S., Ge, M., George, C., and Wang, X.: Contribution of Vehicle Emission and NO2 Surface Conversion to Nitrous Acid (HONO) in Urban Environments: Implications from Tests in a Tunnel, Environ Sci Technol, 10.1021/acs.est.1c00405, 2021a.

Li, X., Brauers, T., Häseler, R., Bohn, B., Fuchs, H., Hofzumahaus, A., Holland, F., Lou, S., Lu, K. D., Rohrer, F., Hu, M., Zeng, L. M., Zhang, Y. H., Garland, R. M., Su, H., Nowak, A., Wiedensohler, A., Takegawa, N., Shao, M., and Wahner, A.: Exploring the atmospheric chemistry of nitrous acid (HONO) at a rural site in Southern China, Atmospheric Chemistry and Physics, 12, 1497-1513, 10.5194/acp-12-1497-2012, 2012.

Li, Y., Wang, X., Wu, Z., Li, L., Wang, C., Li, H., Zhang, X., Zhang, Y., Li, J., Gao, R., Xue, L., Mellouki, A., Ren, Y., and Zhang, Q.: Atmospheric nitrous acid (HONO) in an alternate process of haze pollution and ozone pollution in urban Beijing in summertime: Variations, sources and contribution to atmospheric photochemistry, Atmospheric Research, 260, 10.1016/j.atmosres.2021.105689, 2021b.

Liao, S., Zhang, J., Yu, F., Zhu, M., Liu, J., Ou, J., Dong, H., Sha, Q., Zhong, Z., Xie, Y., Luo, H., Zhang, L., and Zheng, J.: High Gaseous Nitrous Acid (HONO) Emissions from Light-Duty Diesel Vehicles, Environ Sci Technol, 55, 200-208, 10.1021/acs.est.0c05599, 2021.

Liu, J., Deng, H., Li, S., Jiang, H., Mekic, M., Zhou, W., Wang, Y., Loisel, G., Wang, X., and Gligorovski, S.: Light-enhanced heterogeneous conversion of NO2 to HONO on solid films consisted of fluorene and fluorene/Na2SO4: An impact on urban and indoor atmosphere, Environ Sci Technol, 10.1021/acs.est.0c02627, 2020a.

Liu, J., Liu, Z., Ma, Z., Yang, S., Yao, D., Zhao, S., Hu, B., Tang, G., Sun, J., Cheng, M., Xu, Z., and Wang, Y.: Detailed budget analysis of HONO in Beijing, China: Implication on atmosphere

oxidation capacity in polluted megacity, Atmospheric Environment, 244, 10.1016/j.atmosenv.2020.117957, 2021.

Liu, Y., Han, C., Ma, J., Bao, X., and He, H.: Influence of relative humidity on heterogeneous kinetics of NO2 on kaolin and hematite, Phys Chem Chem Phys, 17, 19424-19431, 10.1039/c5cp02223a, 2015.

Liu, Y., Nie, W., Xu, Z., Wang, T., Wang, R., Li, Y., Wang, L., Chi, X., and Ding, A.: Semi-quantitative understanding of source contribution to nitrous acid (HONO) based on 1 year of continuous observation at the SORPES station in eastern China, Atmospheric Chemistry and Physics, 19, 13289-13308, 10.5194/acp-19-13289-2019, 2019a.

Liu, Y., Ni, S., Jiang, T., Xing, S., Zhang, Y., Bao, X., Feng, Z., Fan, X., Zhang, L., and Feng, H.: Influence of Chinese New Year overlapping COVID-19 lockdown on HONO sources in Shijiazhuang, Sci Total Environ, 745, 141025, 10.1016/j.scitotenv.2020.141025, 2020b.

Liu, Y., Lu, K., Li, X., Dong, H., Tan, Z., Wang, H., Zou, Q., Wu, Y., Zeng, L., Hu, M., Min, K. E., Kecorius, S., Wiedensohler, A., and Zhang, Y.: A Comprehensive Model Test of the HONO Sources Constrained to Field Measurements at Rural North China Plain, Environ Sci Technol, 53, 3517-3525, 10.1021/acs.est.8b06367, 2019b.

Liu, Y., Zhang, Y., Lian, C., Yan, C., Feng, Z., Zheng, F., Fan, X., Chen, Y., Wang, W., Chu, B., Wang, Y., Cai, J., Du, W., Daellenbach, K. R., Kangasluoma, J., Bianchi, F., Kujansuu, J., Petäjä, T., Wang, X., Hu, B., Wang, Y., Ge, M., He, H., and Kulmala, M.: The promotion effect of nitrous acid on aerosol formation in wintertime in Beijing: the possible contribution of traffic-related emissions, Atmospheric Chemistry and Physics, 20, 13023-13040, 10.5194/acp-20-13023-2020, 2020c.

Liu, Z., Wang, Y., Costabile, F., Amoroso, A., Zhao, C., Huey, L. G., Stickel, R., Liao, J., and Zhu, T.: Evidence of aerosols as a media for rapid daytime HONO production over China, Environ Sci Technol, 48, 14386-14391, 10.1021/es504163z, 2014.

Meng, F., Qin, M., Tang, K., Duan, J., Fang, W., Liang, S., Ye, K., Xie, P., Sun, Y., Xie, C., Ye, C., Fu, P., Liu, J., and Liu, W.: High-resolution vertical distribution and sources of HONO and NO2 in the nocturnal boundary layer in urban Beijing, China, Atmospheric Chemistry and Physics, 20, 5071-5092, 10.5194/acp-20-5071-2020, 2020.

Meusel, H., Tamm, A., Kuhn, U., Wu, D., Leifke, A. L., Fiedler, S., Ruckteschler, N., Yordanova, P., Lang-Yona, N., Pöhlker, M., Lelieveld, J., Hoffmann, T., Pöschl, U., Su, H., Weber, B., and Cheng, Y.: Emission of nitrous acid from soil and biological soil crusts represents an important source of HONO in the remote atmosphere in Cyprus, Atmospheric Chemistry and Physics, 18, 799-813, 10.5194/acp-18-799-2018, 2018.

Peng, Q., Palm, B. B., Melander, K. E., Lee, B. H., Hall, S. R., Ullmann, K., Campos, T., Weinheimer, A. J., Apel, E. C., Hornbrook, R. S., Hills, A. J., Montzka, D. D., Flocke, F., Hu, L., Permar, W., Wielgasz, C., Lindaas, J., Pollack, I. B., Fischer, E. V., Bertram, T. H., and Thornton, J. A.: HONO Emissions from Western U.S. Wildfires Provide Dominant Radical Source in Fresh Wildfire Smoke, Environ Sci Technol, 54, 5954-5963, 10.1021/acs.est.0c00126, 2020.

R. Kurtenbach, K.H. Becker, J.A.G. Gomes, J. Kleffmann, J.C. L.orzer, M. Spittler, P. Wiesen, R. Ackermann, A. Geyer, and Platt, U.: Investigations of emissions and heterogeneous formation of HONO in a road traffic tunnel, Atmospheric Environment, , 3385–3394, 2001.

Ren, Y., Stieger, B., Spindler, G., Grosselin, B., Mellouki, A., Tuch, T., Wiedensohler, A., and Herrmann, H.: Role of the dew water on the ground surface in HONO distribution: a case measurement in Melpitz, Atmospheric Chemistry and Physics, 20, 13069-13089, 10.5194/acp-20-13069-2020, 2020.

Saunders, S. M., Jenkin, M. E., Derwent, R. G., and Pilling, M. J.: Protocol for the development of the Master Chemical Mechanism, MCM v3 (Part A): tropospheric degradation of non-aromatic volatile organic compounds, Atmos Chem Phys, 10.5194/acpd-2-1847-2002, 2003.

Shi, X., Ge, Y., Zheng, J., Ma, Y., Ren, X., and Zhang, Y.: Budget of nitrous acid and its impacts on atmospheric oxidative capacity at an urban site in the central Yangtze River Delta region of China, Atmospheric Environment, 238, 10.1016/j.atmosenv.2020.117725, 2020.

Song, Y., Zhang, Y., Xue, C., Liu, P., He, X., Li, X., and Mu, Y.: The seasonal variations and potential sources of nitrous acid (HONO) in the rural North China Plain, Environ Pollut, 311, 119967, 10.1016/j.envpol.2022.119967, 2022.

Sun, J., Shen, Z., Zeng, Y., Niu, X., Wang, J., Cao, J., Gong, X., Xu, H., Wang, T., Liu, H., and Yang, L.: Characterization and cytotoxicity of PAHs in PM2.5 emitted from residential solid fuel burning in the Guanzhong Plain, China, Environ Pollut, 241, 359-368, 10.1016/j.envpol.2018.05.076, 2018.

Sun, J., Shen, Z., Cao, J., Zhang, L., Wu, T., Zhang, Q., Yin, X., Lei, Y., Huang, Y., Huang, R. J., Liu, S., Han, Y., Xu, H., Zheng, C., and Liu, P.: Particulate matters emitted from maize straw burning for winter heating in rural areas in Guanzhong Plain, China: Current emission and future reduction, Atmospheric Research, 184, 66-76, 10.1016/j.atmosres.2016.10.006, 2017.

Tang, M.-X., He, L.-Y., Xia, S.-Y., Jiang, Z., He, D.-Y., Guo, S., Hu, R.-Z., Zeng, H., and Huang, X.-F.: Coarse particles compensate for missing daytime sources of nitrous acid and enhance atmospheric oxidation capacity in a coastal atmosphere, Science of The Total Environment, 915, 10.1016/j.scitotenv.2024.170037, 2024.

Tong, S., Hou, S., Zhang, Y., Chu, B., Liu, Y., He, H., Zhao, P., and Ge, M.: Comparisons of measured nitrous acid (HONO) concentrations in a pollution period at urban and suburban Beijing, in autumn of 2014, Science China Chemistry, 58, 1393-1402, 10.1007/s11426-015-5454-2, 2015.

Tong, S., Hou, S., Zhang, Y., Chu, B., Liu, Y., He, H., Zhao, P., and Ge, M.: Exploring the nitrous acid (HONO) formation mechanism in winter Beijing: direct emissions and heterogeneous production in urban and suburban areas, Faraday Discuss, 189, 213-230, 10.1039/c5fd00163c, 2016.

VandenBoer, T. C., Young, C. J., Talukdar, R. K., Markovic, M. Z., Brown, S. S., Roberts, J. M., and Murphy, J. G.: Nocturnal loss and daytime source of nitrous acid through reactive uptake and displacement, Nature Geoscience, 8, 55-60, 10.1038/ngeo2298, 2014.

Weber, B., Wu, D., Tamm, A., Ruckteschler, N., Rodriguez-Caballero, E., Steinkamp, J., Meusel, H., Elbert, W., Behrendt, T., Sorgel, M., Cheng, Y., Crutzen, P. J., Su, H., and Poschl, U.: Biological

soil crusts accelerate the nitrogen cycle through large NO and HONO emissions in drylands, Proc Natl Acad Sci U S A, 112, 15384-15389, 10.1073/pnas.1515818112, 2015.

Wu, D., Horn, M. A., Behrendt, T., Muller, S., Li, J., Cole, J. A., Xie, B., Ju, X., Li, G., Ermel, M., Oswald, R., Frohlich-Nowoisky, J., Hoor, P., Hu, C., Liu, M., Andreae, M. O., Poschl, U., Cheng, Y., Su, H., Trebs, I., Weber, B., and Sorgel, M.: Soil HONO emissions at high moisture content are driven by microbial nitrate reduction to nitrite: tackling the HONO puzzle, ISME J, 13, 1688-1699, 10.1038/s41396-019-0379-y, 2019.

Xing, C., Xu, S., Song, Y., Liu, C., Liu, Y., Lu, K., Tan, W., Zhang, C., Hu, Q., Wang, S., Wu, H., and Lin, H.: A new insight into the vertical differences in NO2 heterogeneous reaction to produce HONO over inland and marginal seas, Atmospheric Chemistry and Physics, 23, 5815-5834, 10.5194/acp-23-5815-2023, 2023.

Xu, Z., Wang, T., Wu, J., Xue, L., Chan, J., Zha, Q., Zhou, S., Louie, P. K. K., and Luk, C. W. Y.: Nitrous acid (HONO) in a polluted subtropical atmosphere: Seasonal variability, direct vehicle emissions and heterogeneous production at ground surface, Atmospheric Environment, 106, 100-109, 10.1016/j.atmosenv.2015.01.061, 2015.

Xue, C.: Substantially Growing Interest in the Chemistry of Nitrous Acid (HONO) in China: Current Achievements, Problems, and Future Directions, Environ Sci Technol, 10.1021/acs.est.2c02237, 2022.

Xue, C., Zhang, C., Ye, C., Liu, P., Catoire, V., Krysztofiak, G., Chen, H., Ren, Y., Zhao, X., Wang, J., Zhang, F., Zhang, C., Zhang, J., An, J., Wang, T., Chen, J., Kleffmann, J., Mellouki, A., and Mu, Y.: HONO Budget and Its Role in Nitrate Formation in the Rural North China Plain, Environmental Science & Technology, 54, 11048-11057, 10.1021/acs.est.0c01832, 2020.

Ye, C., Lu, K., Ma, X., Qiu, W., Li, S., Yang, X., Xue, C., Zhai, T., Liu, Y., Li, X., Li, Y., Wang, H., Tan, Z., Chen, X., Dong, H., Zeng, L., Hu, M., and Zhang, Y.: HONO chemistry at a suburban site during the EXPLORE-YRD campaign in 2018: formation mechanisms and impacts on O3 production, Atmospheric Chemistry and Physics, 23, 15455-15472, 10.5194/acp-23-15455-2023, 2023.

Yu, Y., Cheng, P., Li, H., Yang, W., Han, B., Song, W., Hu, W., Wang, X., Yuan, B., Shao, M., Huang, Z., Li, Z., Zheng, J., Wang, H., and Yu, X.: Budget of nitrous acid (HONO) at an urban site in the fall season of Guangzhou, China, Atmospheric Chemistry and Physics, 22, 8951-8971, 10.5194/acp-22-8951-2022, 2022.

Zhan, Y., Luo, Y., Deng, X., Zhang, K., Zhang, M., Grieneisen, M. L., and Di, B.: Satellite-Based Estimates of Daily NO(2) Exposure in China Using Hybrid Random Forest and Spatiotemporal Kriging Model, Environ Sci Technol, 52, 4180-4189, 10.1021/acs.est.7b05669, 2018.

Zhang, J., An, J., Qu, Y., Liu, X., and Chen, Y.: Impacts of potential HONO sources on the concentrations of oxidants and secondary organic aerosols in the Beijing-Tianjin-Hebei region of China, Sci Total Environ, 647, 836-852, 10.1016/j.scitotenv.2018.08.030, 2019a.

Zhang, J., Chen, J., Xue, C., Chen, H., Zhang, Q., Liu, X., Mu, Y., Guo, Y., Wang, D., Chen, Y., Li,

J., Qu, Y., and An, J.: Impacts of six potential HONO sources on HOx budgets and SOA formation during a wintertime heavy haze period in the North China Plain, Sci Total Environ, 681, 110-123, 10.1016/j.scitotenv.2019.05.100, 2019b.

Zhang, L., Wang, T., Zhang, Q., Zheng, J., Xu, Z., and Lv, M.: Potential sources of nitrous acid (HONO) and their impacts on ozone: A WRF-Chem study in a polluted subtropical region, Journal of Geophysical Research: Atmospheres, 121, 3645-3662, 10.1002/2015jd024468, 2016.

Zhang, Q., Liu, P., George, C., Chen, T., Ren, Y., Mu, Y., Song, M., Herrmann, H., Mellouki, A., Chen, J., Zhao, X., and Zeng, Y.: Unveiling the underestimated direct emissions of nitrous acid (HONO), Proceedings of the National Academy of Sciences, 120, 10.1073/pnas, 2023.

Zhang, W., Tong, S., Ge, M., An, J., Shi, Z., Hou, S., Xia, K., Qu, Y., Zhang, H., Chu, B., Sun, Y., and He, H.: Variations and sources of nitrous acid (HONO) during a severe pollution episode in Beijing in winter 2016, Sci Total Environ, 648, 253-262, 10.1016/j.scitotenv.2018.08.133, 2019c.

Zhang, W., Tong, S., Jia, C., Wang, L., Liu, B., Tang, G., Ji, D., Hu, B., Liu, Z., Li, W., Wang, Z., Liu, Y., Wang, Y., and Ge, M.: Different HONO Sources for Three Layers at the Urban Area of Beijing, Environ Sci Technol, 54, 12870-12880, 10.1021/acs.est.0c02146, 2020.

Zhang, X., Tong, S., Jia, C., Zhang, W., Li, J., Wang, W., Sun, Y., Wang, X., Wang, L., Ji, D., Wang, L., Zhao, P., Tang, G., Xin, J., Li, A., and Ge, M.: The Levels and Sources of Nitrous Acid (HONO) in Winter of Beijing and Sanmenxia, Journal of Geophysical Research: Atmospheres, 127, 10.1029/2021jd036278, 2022.

Zheng, J., Shi, X., Ma, Y., Ren, X., Jabbour, H., Diao, Y., Wang, W., Ge, Y., Zhang, Y., and Zhu, W.: Contribution of nitrous acid to the atmospheric oxidation capacity in an industrial zone in the Yangtze River Delta region of China, Atmospheric Chemistry and Physics, 20, 5457-5475, 10.5194/acp-20-5457-2020, 2020.

Zhou, X., Zhang, N., TerAvest, M., Tang, D., Hou, J., Bertman, S., Alaghmand, M., Shepson, P. B., Carroll, M. A., Griffith, S., Dusanter, S., and Stevens, P. S.: Nitric acid photolysis on forest canopy surface as a source for tropospheric nitrous acid, Nature Geoscience, 4, 440-443, 10.1038/ngeo1164, 2011.